43rd AIAA/ASME/SAE/ASEE Joint Propulsion Conference & Exhibit
8 - 11 July 2007, Cincinnati, OH

AIAA 2007-5677

Effects of Prandtl Number on Reactive Jets

Fernando S. Costa and César A.V. Salvador
Instituto Nacional de Pesquisas Espaciais, C. Paulista, São Paulo, 12630-000, Brazil

Stephen B. Gabriel
University of Southampton, Southampton, SO171BJ, UK

This work analyses the effects of the Prandtl number on mixture fraction within reactive jets by using the integral method. The velocity and mixture fraction fields of plane and cylindrical jets in the laminar flow regime are determined. It is verified that the ratios of the thicknesses of the momentum and mixture fraction boundary layers obey a simple ordinary differential equation with a standard form, in all cases considered. Integration of this equation for several Re and Pr numbers indicates that the thickness ratio becomes, in general, approximately constant for distances not far from the injector. It is shown that mixture profiles and flame lengths can be significantly affected by differential diffusion of scalars and momentum. As expected, the scalar thicknesses are larger, equal or lower than the momentum thicknesses for Pr > 1, Pr = 1 and Pr < 1, respectively.

Nomenclature

a,c	=	constants
d_i	=	diameter or width of injection
u	=	streamwise velocity component
u_i	=	injection velocity
u_m	=	centerline streamwise velocity
v	=	normal velocity component
F	=	fuel
f	=	mixture fraction
f_m	=	centerline mixture fraction
i	=	species or geometry
x	=	streamwise coordinate
r	=	normal coordinate
O	=	oxidizer
P	=	product
Pr	=	Prandtl number $=\upsilon/\alpha$
T	=	temperature
Y	=	mass fraction
s	=	oxidizer/fuel stoichiometric mass ratio
α	=	species diffusivity or thermal diffusivity
ω	=	ratio of boundary layer thicknesses
$\dot{w}_F'''$	=	fuel consumption rate per unit volume
ΔH	=	heat of reaction per kg of fuel
δ	=	boundary layer thickness
υ	=	dynamic viscosity
ρ	=	mixture density

I. Introduction

Free jets are important in many technological applications and in fundamental studies of inert and reactive flows. Experiments indicate that free jets can present self-similarity beyond 5 or 6 exit diameters from the injector and, consequently, distances, velocities, temperatures and mass fractions in the flow can be scaled up by characteristic length, velocity, temperature and species mass fractions, respectively.

More experimental data is available for the axisymmetric case, since it is easier to setup experimentally an axisymmetric jet than a planar jet, although more theoretical analysis is available for planar cases (Agrawal and Prasad, 2003, Bhat and Narasimha, 1996; Hussein et al., 1994; Wygnanski and Fiedler, 1969).

The usual theoretical approach of free jets is to perform an order of magnitude analysis of the Navier-Stokes equations in the self-similar region. The boundary layer approximation is applied, allowing a significant reduction in the number of terms. The resulting terms are then scaled using the appropriate length, velocity, species mass fraction and temperature scales. Further, by invoking conservation of momentum, the streamwise variation of width, velocity and scalars can be obtained (Tennekes and Lumley, 1972, Schlichting, 1968).

The theory of free jets with a review of theory and experiments was presented by Schlichting (1968), who obtained in 1933 the classical solutions for narrow jets issuing from small slits or holes. Toong (1983) extended Schlichting solution for a planar jet and solved the reactive problem considering the effects of compressibility and Prandtl number, *Pr*, i.e., the effects of differential diffusion of heat and momentum.

The integral method has been used to obtain approximate solutions for the boundary layer equations, being especially useful when exact analytical solutions are not available. In general, Gaussian or polynomial similar profiles for the axial velocity and scalar fields are chosen to integrate the conservation equations and $Pr = 1$ is adopted. Steiger and Bloom (1963) applied the integral method, assuming polynomial profiles, to solve the momentum equations for 2D laminar jets and wakes. Kanury (1975) assumed linear profiles of velocity and temperature and used the integral method to obtain approximate solutions, for inert and reactive jets issuing from finite slits or holes, in planar and cylindrical geometries.

The objective of this work is to analyse the effects of *Pr* on reactive jets, by using the integral method. The problem is solved for planar and cylindrical geometries, both in the laminar flow regime. The analysis is made for slits or holes of finite size, considering similar polynomial profiles of the velocity and scalar fields. Analytical or semi-analytical expressions are obtained for the velocity and mixture fraction in terms of *Pr*. It is shown that the ratio of the mixture fraction thickness to the momentum thickness in all cases obey a relatively simple differential equation with a standard form. Integration of this equation indicates that the mixture fraction profiles of reactive jets can be significantly affected by differential diffusion.

II. Governing Equations and Boundary Conditions

A single step chemical reaction is considered in the analysis:

$$1\text{ kg } F + s\text{ kg } O \rightarrow (1+s)\text{ kg } P + \Delta\text{H J/kg fuel} \tag{1}$$

Assuming equal species and thermal diffusivities ($Le = 1$), the mass, momentum, species and energy boundary layer equations are given, respectively, by:

$$\left(r^n u\right)_x + \left(r^n v\right)_r = 0 \tag{2}$$

$$r^n u u_x + r^n v u_r = \upsilon\left(r^n u_r\right)_r \tag{3}$$

$$r^n u Y_{i,x} + r^n v Y_{i,r} = \alpha\left(r^n Y_{i,r}\right)_r + r^n \dot{w}_i''' / \rho \text{ , } i = \text{F,O, P} \tag{4}$$

$$r^n u\left(T - T_\infty\right)_x + r^n v\left(T - T_\infty\right)_r = \alpha\left(r^n\left(T - T_\infty\right)_r\right)_r - r^n \Delta\text{H}\dot{w}_F''' / \rho \tag{5}$$

where $n = 0, 1$ for plane and cylindrical jets, respectively. Equations (4) and (5) can be combined, yielding:

$$r^n u f_x + r^n v f_r = \alpha\left(r^n f_r\right)_r \tag{6}$$

where

$$f = \frac{sY_F - Y_O + Y_{O,\infty}}{sY_{F,i} + Y_{O,\infty}} = \frac{T - T_\infty + \Delta H Y_F}{T_i - T_\infty + \Delta H Y_{F,i}} = \frac{(s+1)Y_F + Y_P - \left(1 - Y_{O,\infty}\right)}{(s+1)Y_{F,i} - \left(1 - Y_{O,\infty}\right)} \tag{7}$$

The variable f is called the mixture fraction and, usually, has values between 0 and 1. Boundary conditions for u and f are

$$r = \delta_F,\ 0 \le x \le \infty,\ f = f_r = f_{rr} = 0 \tag{8a}$$

$$r = \delta_H,\ 0 \le x \le \infty,\ u = u_r = u_{rr} = 0 \tag{8b}$$

$$r = 0,\ 0 \le x \le \infty,\ u_r = f_r = 0 \tag{8c}$$

$$x = 0,\ 0 \le r \le d_i/2,\ f = 1,\ u = u_i \tag{8d}$$

$$x = \infty,\ 0 \le r \le \infty,\ u = u_r = f = f_r = 0 \tag{8e}$$

where δ_F and δ_H are the mixture fraction and the momentum boundary layer thicknesses and d_i is the injector exit diameter of a round jet, or injector exit width of a plane jet. The boundary layer thicknesses are defined by the points where the longitudinal velocity are a small fraction, e.g., 0.1 or 1 %, of the centerline velocity. It should be noted that derivatives of Eqs. (3) and (6) with respect to r can provide additional conditions at the boundary layers' edges.

Next, the mass, momentum and mixture fraction equations are integrated from the flow centerline to the jet boundary δ_i and to an arbitrary position $\psi\delta_i$ inside the boundary layer, with $\psi \in [0,1]$. This approach has been adopted previously by Moses (1968) and Kanury (1975). Similar velocity and scalar profiles are assumed and substituted into the integrated equations, yielding expressions describing the velocity and scalar fields. Some of these expressions will require the numerical solution of ordinary differential equations of a standard form.

III. Integration of the Mass and Momentum Equations

Equations (2) and (3) can be integrated in the interval $r = (0, \psi\delta_H)$, yielding, respectively:

$$v_{\psi\delta_H} = -\frac{1}{\left(\psi\delta_H\right)^n} \frac{\partial}{\partial x} \int_0^{\psi\delta_H} r^n u\, dr \tag{9}$$

$$\frac{\partial}{\partial x} \int_0^{\psi\delta_H} r^n u^2 dr + \left[r^n uv\right]_{\psi\delta_H} = \left[\nu r^n \frac{\partial u}{\partial r}\right]_{\psi\delta_H} \tag{10}$$

Polynomial profiles of velocities, satisfying boundary conditions given by Eqs. (8b-e), are considered to solve Eqs. (9) and (10):

$$u/u_m = \sum_{i=0}^{k} \gamma_i \left(r/\delta_H\right)^i \tag{11}$$

where $u_m = u_m\left(x\right)$ is the velocity at r = 0. The polynomial coefficients, γ_i, of order up to order k = 4 are shown on Table 1. It should be noted that polynomials of lower order do not satisfy all derivative conditions. Alternatively, linear combinations of the basic polynomials could be adjusted to experiments.

Table 1. Polynomial coefficients for similarity profiles up to 4th order.

Pol. order	γ_0	γ_1	γ_2	γ_3	γ_4
1	+1	–1	0	0	0
2	+1	0	–1	0	0
3	+1	0	–3	+2	0
4	+1	0	–6	+8	–3

Using Eq. (11), the velocity u and its derivative at $\psi\delta_H$ are given, respectively, by

$$u\left(\psi\delta_H\right) = c_4 u_m \tag{12a}$$

$$\frac{\partial u}{\partial r}\left(\psi\delta_H\right) = c_3 \frac{u_m}{\delta_H} \tag{12b}$$

where $c_4 = \sum_{i=0}^{k} \gamma_i \psi^i$ and $c_3 = \sum_{i=1}^{k} i\gamma_i \psi^{i-1}$ are constants. In order to solve Eqs. (9) and (10) the following integrals are required:

$$\int_0^{\delta_H} r^n u dr = c_{11} u_m \delta_H^{n+1} \quad ; \quad \int_0^{\psi\delta_H} r^n u dr = c_{12} u_m \delta_H^{n+1} \tag{13a,b}$$

$$\int_0^{\delta_H} r^n u^2 dr = c_{21} u_m^2 \delta_H^{n+1} \quad ; \quad \int_0^{\psi\delta_H} r^n u^2 dr = c_{22} u_m^2 \delta_H^{n+1} \tag{13c,d}$$

where $c_{11} = \int_0^1 \sum_{i=0}^{k} \gamma_i z^{i+n} dz$, $c_{12} = \int_0^{\psi} \sum_{i=0}^{k} \gamma_i z^{i+n} dz$, $c_{21} = \int_0^1 z^n \left(\sum_{i=0}^{k} \gamma_i z^i\right)^2 dz$ and $c_{22} = \int_0^{\psi} z^n \left(\sum_{i=0}^{k} \gamma_i z^i\right)^2 dz$.

Substituting Eq. (13b) into Eq. (9), yields:

$$v_{\psi\delta_H} = -\frac{c_{12}}{\left(\psi\delta_H\right)^n} \frac{d}{dx}\left(u_m \delta_H^{n+1}\right) \tag{14}$$

and, for ψ = 1, it follows that

$$v_{\delta_H} = -\frac{c_{11}}{\delta_H^n} \frac{d}{dx}\left(u_m \delta_H^{n+1}\right) \tag{15}$$

Note that standard derivatives can be used, since u_m and δ_H depend only on x. Solving Eq. (10) for ψ = 1, gives

$$\frac{\partial}{\partial x}\int_0^{\delta_H} r^n u^2 dr = \frac{\partial}{\partial x}\left(c_{21} u_m^2 \delta_H^{n+1}\right) = 0 \tag{16}$$

which indicates that the jet streamwise momentum is constant, a well-known classical result. Therefore,

$$u_m^2 \delta_H^{n+1} = u_i^2 \left(d_i/2\right)^{n+1} = \text{constant} = C \tag{17}$$

and

$$\delta_H = \left(C/u_m^2\right)^{\frac{1}{n+1}} \tag{18}$$

Solving Eq. (10) for an arbitrary position $\psi\delta_H$ inside the viscous boundary layer, yields

$$\frac{d}{dx}\left(u_m \delta_H^{n+1}\right) = -\frac{c_3}{c_4 c_{12}} \upsilon \psi^n \delta_H^{n+1} \tag{19}$$

Then, substituting Eq. (18) into Eq. (19) and simplifying, it yields:

$$u_m / u_i = X^p \tag{20}$$

where $X = 1 + \frac{c_5}{\mathrm{Re}} \frac{x}{d_i}$, with $c_5 = \frac{4}{p} \frac{c_3 \psi^n}{c_4 c_{12}}$ and $p = \frac{n+1}{n-3}$.

Consequently, u_m decays with distance from the injection hole or slit, with $p = -1$ for a cylindrical jet and $p = -1/3$ for a planar jet, as already shown by Schlichting (1968). It should be noted that c_5 depends on ψ and n and that $c_5 > 0$, since $c_3 < 0$. A proper ψ value can be also chosen to adjust to experimental data. At distances far from the injector, where the similarity solutions are valid, $\left(c_5/\mathrm{Re}\right)\left(x/d_i\right) >> 1$, therefore, $u_m/u_i \cong c_5^p \left(x/\mathrm{Re}\, d_i\right)^p$, and c_5^p indicates the decay rate of the centerline velocity for a given similar profile and for a given ψ value. Figure 1 shows the influence of ψ on c_5^p for plane and cylindrical jets, considering polynomial profiles of order up to 4. Kanury (1975) has found previously c_5^p assuming ψ = 0.5 and a linear profile.

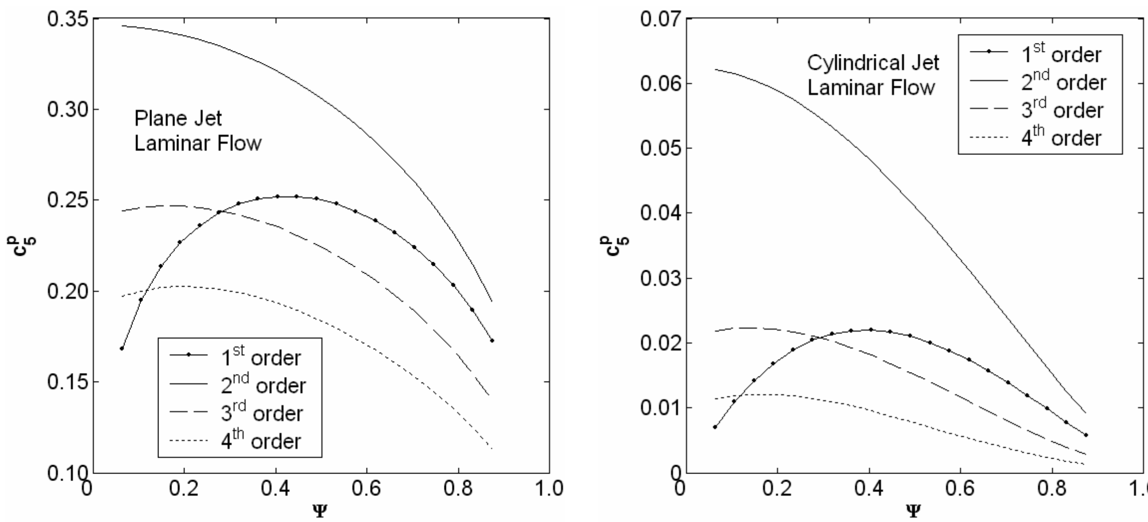

Figure 1. Effects of ψ and polynomial order on c_5^p for plane and cylindrical laminar jets.

Substituting u_m into Eq. (18) it follows that

$$2\delta_H / d_i = X^{2/(3-n)} \tag{21}$$

Therefore the width, $2\delta_H$, of a free circular jet grows linearly and the thickness of a plane jet increases with $x^{2/3}$.

The spreading angle is given by $\theta = 2\tan^{-1}\frac{d\delta_H}{dx} = 2\tan^{-1}\left[\frac{c_5}{(3-n)\mathrm{Re}}\left(\frac{c_5 x}{\mathrm{Re}\, d_i}\right)^{\frac{n-1}{3-n}}\right]$, indicating that it depends on *Re*. The normal velocity component is obtained from Eqs. (15), (20) and (21):

$$\frac{v_{\delta_H}}{u_i} = \frac{n+1}{n-3}\frac{c_{11}}{2}\frac{c_5}{\mathrm{Re}} X^{2/(n-3)} \tag{22}$$

IV. Integration of the Mixture Fraction Equation

Equation (6) for mixture fraction balance, can be integrated up to an arbitrary position inside the mixture fraction layer, $r = (0, \psi_F \delta_F)$, where $\psi_F \in [0,1]$, yielding:

$$\frac{\partial}{\partial x}\int_0^{\psi_F\delta_F} r^n u dr + \left[r^n v f\right]_{\psi_F\delta_F} = \left[\alpha r^n \frac{\partial f}{\partial r}\right]_{\psi_F\delta_F} \tag{23}$$

Polynomial profiles were also considered to solve Eq. (23):

$$f / f_m = \sum_{i=0}^{k} \kappa_i \left(r/\delta_F\right)^i \tag{24}$$

is a polynomial profile of mixture fraction, satisfying boundary conditions given by Eqs. (8a-e), with coefficients $\kappa_i \equiv \gamma_i$. The ratio between the mixture fraction layer thickness and the viscous layer thickness is defined by

$$\omega = \delta_F / \delta_H \tag{25}$$

Substituting the polynomial profiles into Eq. (23) and making several mathematical manipulations, the following expression is obtained for the boundary layers thickness ratio:

$$\frac{d\omega}{dX} = \frac{c_{11}X^{-1}}{A_\omega}\left(\frac{1+n}{3-n}B_\omega + \frac{a_3}{\mathrm{Pr}}\right) \tag{26}$$

where A_ω and B_ω are functions of ω, $a_3 = 4a_2\psi_F^n / (c_5 c_{11})$ and $a_2 = \sum_{i=1}^{k} ik_i\psi_F^{i-1}$.

V. Results

Equation (26) was integrated for several Re and Pr numbers and for several $\psi = \psi_F$ values, using a stiff solver.

Figure 2 shows the effects of polynomial order on ω for cylindrical jets, for $Pr = 0.7$ and $Pr = 1.4$. It is seen that the polynomial order does not affect significantly ω in both cases.

Figure 3 shows the effects of ψ_F values on ω for a cylindrical jet and using a 4th order polynomial. It was found that a fourth order polynomial with $\psi_F = 0.074$ fits reasonably well the experimental radial velocity profiles.

Figure 4 shows the effects of Re on ω. It is seen that larger Re values increase ω values, and that, for Re > 100, ω has a constant value just after injection, and the jets become turbulent.

Figure 5 shows the effects of Pr on ω. It is verified that ω is larger than unity for Pr < 1 and smaller than unity for Pr > 1, as expected.

Since mixture fraction is affected by Pr, the stoichiometric mixture fraction and the flame length, which depend on reactants stoichiometry, will be affected as well.

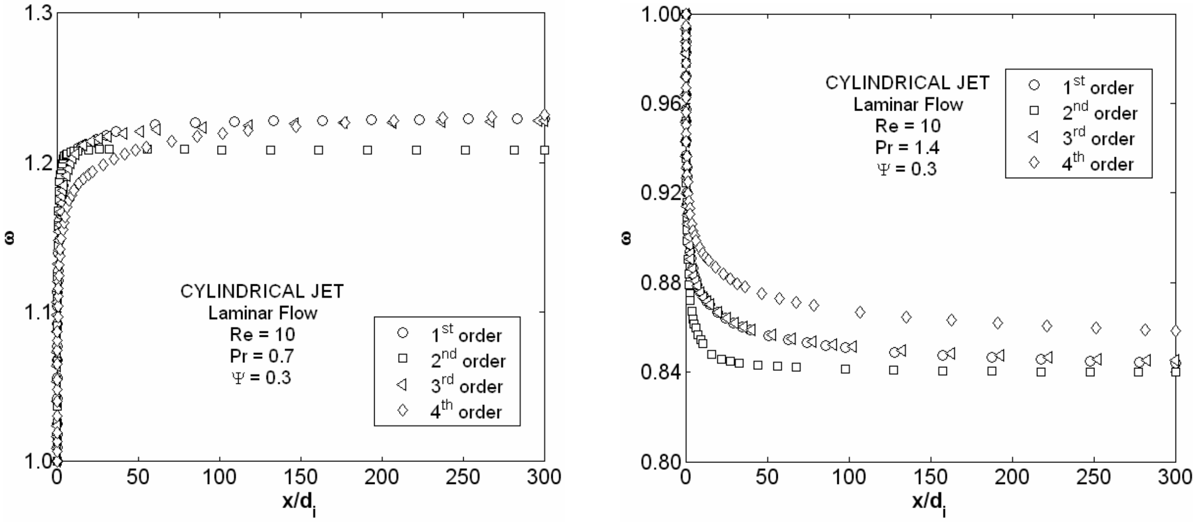

Figure 2. Effects of polynomial order on ω for cylindrical jets.

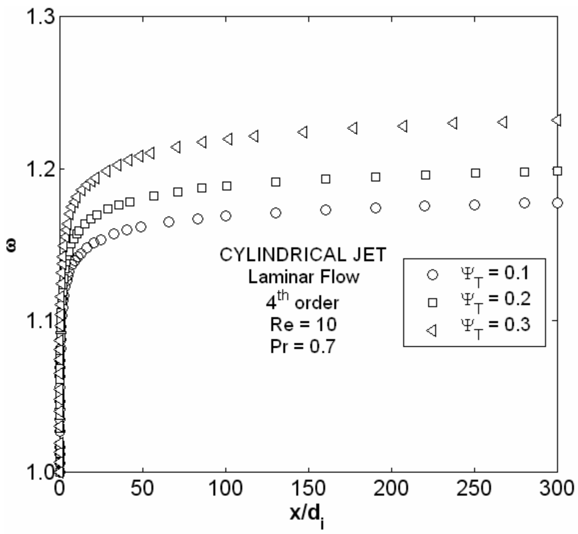

Figure 3. Effects of $\psi_F = \psi$ on ω.

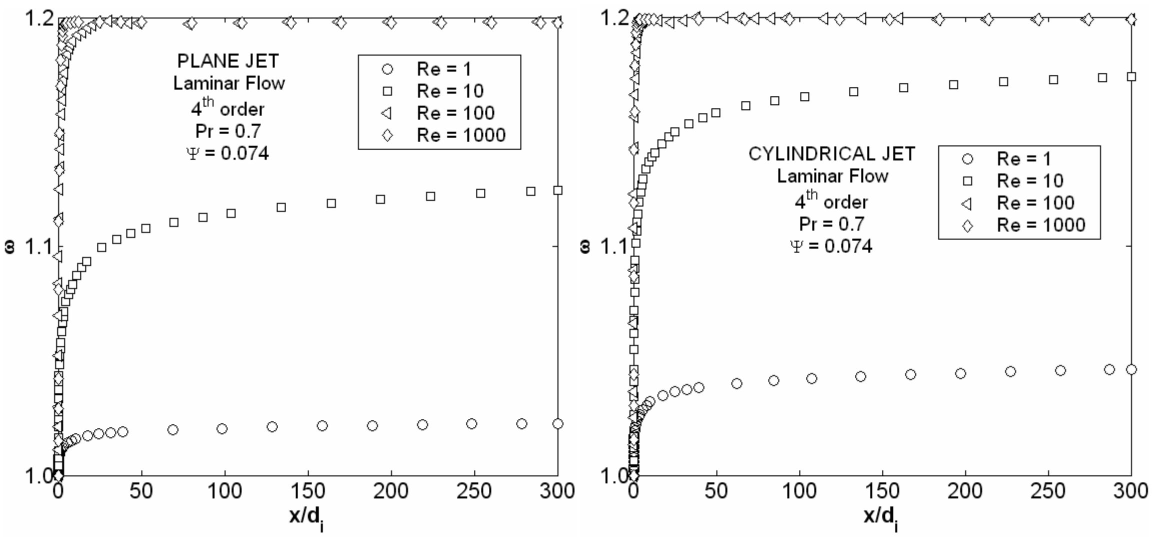

Figure 4. Effects of Re on ω.

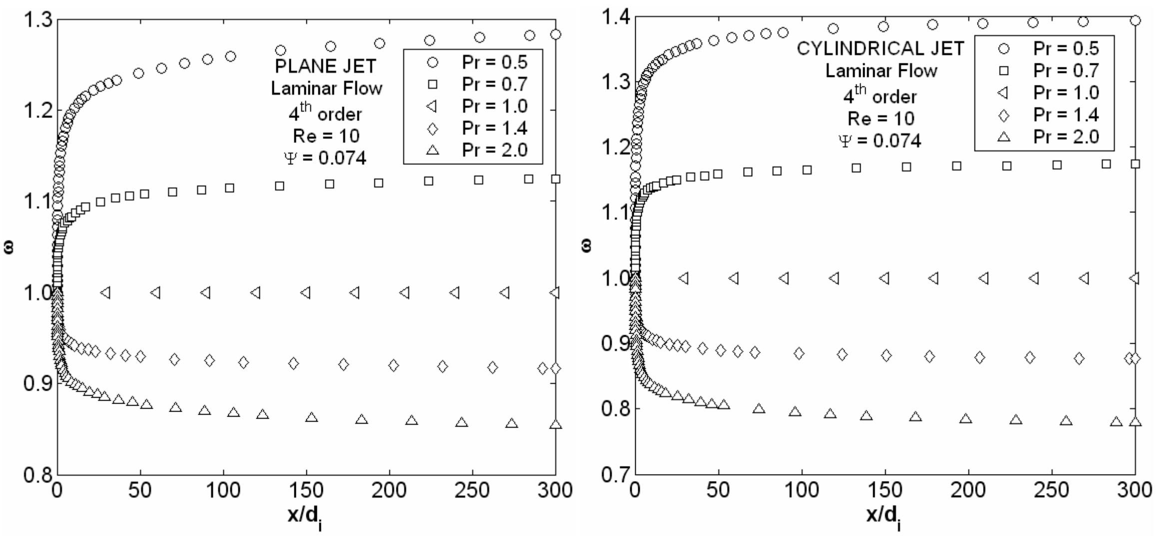

Figure 5. Effects of Pr on ω.

VI. Conclusion

This work described an integral solution with polynomial profiles valid in the developed region for the reactive laminar jet problem, in terms of *Re* and *Pr* numbers, with integration up to boundary edges and up to arbitrary positions inside the viscous and mixture fraction boundary layers and to the boundary edges. It was verified a strong influence of *Re* and *Pr* on mixture fraction thickness and that fourth order polynomial profiles, integrated up to ψ_F = 0.074, yield the best results for the radial profiles. Other reactive jet characteristics, such as jet width, jet spread angle, flame lengths and shapes, and turbulent jets also can be analysed with this approach.

References

Agrawal, A., Prasad, A.K., "Integral Solution for the Mean Flow Profiles of Turbulent Jets, Plumes, and Wakes", *J. Fluids Engineering*, Vol. 125, pp 813-822, Sep 2003.

Bhat, G.S., Narasimha, R.,A., "Volumetrically Heated Jet: Large Eddy Structure and Entrainment Characteristics", *J. Fluid Mech.*, 325, pp. 303–330, 1996.

Carazzo, G., Kaminski, E., Tait, S., "The Route to Self-Similarity in Turbulent Jets and Plumes", *J. Fluid Mech.*, vol. 547, pp. 137–148, 2006.

Corrsin, S., Uberoi, M.S., “Further Experiments on the Flow and Heat Transfer in a Heated Turbulent Air Jet”, NACA Report 998, 1950.

Gutmark, E., and Wygnanski, I., “The Planar Turbulent Jet”, *J. Fluid Mech.*, 73, 1976, pp. 465–495.

Hinze, J.O., *Turbulence*, 2nd ed., McGraw Hill, New York, 1975, pp 534-546.

Hussein, H.J., Capp, S.P., George, W.K., “Velocity Measurements in a High Reynolds Number, Momentum-Conserving Axisymmetric Turbulent Jet”, J. Fluid Mech., 258, 1994, pp. 31–75.

Kanury, A.M., *Introduction to Combustion Phenomena*, Gordon and Breach Publishers, New York, 1975, Chapter 7.

Mi, J., Nobes, D.S., Nathan, G.J., Influence of Jet Exit Conditions on the Passive Scalar Field of an Axisymmetric Free Jet, *J. Fluid Mech.*, vol. 432, 2001, pp. 91-125.

Moses, H.L., “A Strip-Integral Method for Predicting the Behavior of Turbulent Boundary Layers,” *Proc. AFOSR-IFP-Stanford Conference on Computation of Turbulent Boundary Layers*, Stanford University, Palo Alto, Calif., 1968.

Tennekes, H., and Lumley, J.L., *A First Course in Turbulence*, MIT Press, Cambridge, MA, 1972, pp. 127–142.

Toong, T.Y., *Combustion Dynamics*, Mac-Graw-Hill, New York, 1983, pp.73-82.

Schlichting, H., *Boundary-Layer Theory*, 6th Ed., McGraw-Hill, New York, 1968, pp 170-174.

Steiger, M.H., Bloom, M.H., “Integral Method Solutions of Laminar Viscous Free-Mixing”, *AIAA Journal*, Vol. 1, No. 7, 1963, pp 1672-1674.

Wygnanski, I., and Fiedler, H., “Some Measurements in a Self-Preserving Jet”, *J. Fluid Mech.*, 38, 1969, pp. 577–612.